Activation Energies for the Fragmentation of Thiophene Ions by Surface-Induced Dissociation

Hanjo Lim, David G. Schultz, Eric A. Gislason, and Luke Hanley*

Department of Chemistry, m/c 111, University of Illinois at Chicago, Chicago, Illinois 60607-7061

Received: November 25, 1997; In Final Form: March 13, 1998

We have improved our previously described method for extracting activation energies of fragmentation for polyatomic ions from surface-induced dissociation (SID) data [Wainhaus, S. B.; et al. *J. Am. Chem. Soc.* **1997**, *119*, 4001]. Our method analyzes the energy-resolved mass spectra and the kinetic energy distribution spectra of the parent and fragment ions that scatter off the surface. It extracts the activation energies by integrating over the distribution of the initial ion energy and the energy transferred to the surface, taking into account both the average value and the width of these distributions. The new method gave improved activation energies for $SiMe_3^+ \rightarrow SiMe_x^+$ ($x = 0-2$) fragmentation at a hexanethiolate-covered gold surface. We then used our data analysis method to analyze the activation energies for the fragmentation of thiophene ions at the hexanethiolate-covered gold surface. The activation energies for the formation of $C_2H_2S^+$, CHS^+, and $C_3H_3^+$ from $C_4H_4S^+$ were found to be 4.6 ± 0.7, 6.9 ± 0.7, and 6.5 ± 0.7 eV, respectively. Our activation energy results followed the trend in the values from threshold photoelectron photoion coincidence data. However, the SID values were ∼50% higher than the threshold photoelectron photoion coincidence values; this discrepancy mostly resulted from delayed dissociation. This model may be used to extract quantitative activation energies from SID data once certain ongoing issues are resolved in future papers. Molecular dynamics simulations were also performed to assist in the data analysis and to test the assumptions of energy transfer in this system. Qualitative agreement in energy transfer was found between the experiments and simulations.

I. Introduction

When an ion scatters off a surface, its incoming kinetic energy is partitioned among translation, internal excitation, and surface excitation. This energy transfer leads to the surface-induced dissociation (SID) of the scattered ion if its internal excitation exceeds its fragmentation energy. SID is an effective ion activation method for the tandem mass spectrometry of small and large ions including organics, polypeptides, fullerenes, and clusters.[1−5] Photoelectron photoion coincidence, low-energy collision-induced dissociation (CID), blackbody infrared radiative dissociation, high-pressure mass spectrometry, and other methods are available to determine the activation energies of fragmentation for small molecules and ions.[6−11] Some of these methods have also been applied to obtain fragmentation energies for large biological ions, but the accuracy of these large ion fragmentation energies is the subject of ongoing debate. SID has been used to obtain fragmentation energies for both small and large ions.[12−15] SID has three primary advantages for use in determining ion fragmentation energies: (1) it displays an efficient (∼20%) transfer of kinetic to internal energy,[1,16−18] (2) this internal energy is deposited into a relatively narrow distribution,[1,16] and (3) the entire excitation process occurs in a subpicosecond excitation at the surface.[19,20]

We recently described a new method for the extraction of activation energies for scattered fragment ions produced by SID of a parent ion.[12] This method was developed from a hard-sphere atom−diatom gas-phase collision model.[21] It follows closely the approach used by Armentrout and co-workers to treat low-energy CID data.[22] Our method assumes that impulsive excitation dominates SID. It assumes that this excitation can be described by a function that includes as a parameter the activation energy for the formation of the fragment. It subtracts the kinetic energy deposited into the surface from the initial kinetic energy, then it integrates this functional form over the initial kinetic energy distribution. The activation energy is then obtained by comparing the predictions of our method with the energy-resolved mass spectra (ERMS) and kinetic energy distribution spectra (KEDS) of the scattered ions. We tested our method on SID of $SiMe_3^+$ ions at a hexanethiolate-covered Au(111) surface. Our results were close to but lower than the known activation energies by several electronvolts; this discrepancy was due to both limitations in the data analysis method and the accuracy of the experimental data. Close agreement between our experimental data and molecular dynamics simulations demonstrated that impulsive excitation is the dominant excitation mechanism for $SiMe_3^+$ scattering off hexanethiolate-covered gold.[3,23]

This paper is part of an ongoing effort to use SID to obtain accurate fragmentation energies for large biomolecular ions. Our approach is to first develop our method for smaller ions, for which the fragmentation energies are well-known. In this paper, we improve our data analysis method by including the width in the distribution of the energy transferred to the surface and by altering the expression of the data analysis algorithm. We

* Corresponding author. E-mail: LHanley@uic.edu.

S1089-5647(98)00342-3 CCC: $15.00
Published on Web 05/13/1998

test this new method by reanalyzing the SID data for the fragmentation of $SiMe_3^+ \rightarrow SiMe_x^+$ ($x = 0-2$).[12] We then use this method to calculate activation energies for the formation of three fragment ions from the thiophene ion by SID at a hexanethiolate-covered gold surface. We also perform molecular dynamics simulations to assist in the data analysis and to test the assumptions of energy transfer in this system.

II. Experimental Section

The detailed experimental setup and surface preparation can be found in previous papers[3,12,24] and will be only briefly described here. Degassed thiophene was introduced into a 70 eV electron impact ionization source to produce $C_4H_4S^+$. The $C_4H_4S^+$ molecular ion (m/z 84) was mass-selected by a first quadrupole, then guided onto a hexanethiolate (C_6) covered Au(111) surface through a series of dc lenses and a radio frequency octapole ion guide. The ion beam was incident at an angle of 45° off the surface normal. Scattered positive ions were energy- and mass-analyzed by a tandem axial energy analyzer/quadrupole mass spectrometer assembly fixed at 90° from the incident ion beam. The energy distribution of the incident 5−30 eV $C_4H_4S^+$ molecular ion beam was measured as 2.6−4.2 eV (fwhm) by a Faraday cup equipped with a retarding field energy analyzer. The Au crystal temperature was held at 300 K during all scattering experiments. All data were recorded on at least two separate occasions from freshly prepared monolayers to ensure reproducibility and avoid ion beam damage effects.

III. Theory

We have previously described a model for the excitation of a polyatomic ion during SID that is analogous to that used in gas-phase collision-induced dissociation.[12] Our model extracts the activation energy for the formation of a given fragment ion from the plot of the normalized parent and fragment ion signals as a function of the incident ion kinetic energy E. We refer to this plot as the energy-resolved mass spectra (ERMS). Our model treats the polyatomic projectile as a pseudodiatomic species in which one pseudoatom of the diatomic recoils against the other pseudoatom upon impact with the surface pseudoatom. We begin with $P_i(E_t)$, the fraction of molecules with internal energy E_t that dissociates to product channel i before reaching the detector. Averaging this probability of dissociation at a given E over the impact parameter gives the measured SID fraction of products in channel i at that E as given by

$$\begin{aligned} f_i(E) &= 0 \qquad E < A_i \\ &= (E - A_i)^n/[nB_i^{n-1}E] \qquad A_i \le E < A_i + B_i \qquad (1) \\ &= \{E - A_i - [(n-1)B_i/n]\}/E \qquad A_i + B_i \le E \end{aligned}$$

Here, A_i is defined as the threshold or activation energy for the formation of the ith fragment ion from the parent ion; it is the value we wish to obtain from this analysis. $1/B_i$ corresponds to the slope of the dissociation probability near threshold, and n is a fitting constant. A_i, n, and B_i were varied to give the best fit to the experimental data.

One of the limitations of eq 1 is that it cannot account for the observed decrease in the relative intensity of particular fragments with increasing E. To address this shortcoming, we previously proposed expanding the dissociation probability $P_i(E_t)$ implicit in eq 1 in a Taylor series about $E = A_i$ to give a new expression for $f_i(E)$:[12]

$$f_i(E) = [(E - A_i)^2/E]\sum_{k=0}^{\infty} a_{k+1}(E - A_i)^k/a_{i,k+1} \qquad (2)$$

The first two terms of this Taylor series can then be written as

$$\begin{aligned} f_i(E) &= 0 \qquad E < A_i \\ &= [(E - A_i)^2/E][a_i + b_i(E - A_i)] \quad E \ge A_i \qquad (3) \end{aligned}$$

where a_i and b_i are fitting parameters. We expect eq 3 to work well near threshold for simple dissociation processes, and in many cases b_i will be negative.

During the collision, the surface pseudoatom recoils after the collision with the ion and a certain fraction of the initial kinetic energy E is converted into energy of the surface E_{surf}. We previously assumed that each polyatomic ion in the beam with kinetic energy E deposited a fixed amount of energy E_{surf} into the surface. We further assumed that the function $E_{surf}(E)$ was known. Because E_{surf} was not available for internal excitation of the polyatomic ion, we accounted for it simply by subtracting it from the total energy available to the system to dissociate the ion. This gave us an actual fraction of scattered ions in product state i measured at the detector for incident ion energy E as

$$F_i(E) = f_i[E - E_{surf}(E)] \qquad (4)$$

In addition, because eq 4 does not take into account the finite width of our ion beam, we previously described its energy distribution at the nominal beam energy E_0 by

$$P(E; E_0) = (\pi^{1/2}\Delta E)^{-1} \exp[-(E - E_0)^2/\Delta E^2] \qquad (5)$$

where ΔE is estimated from the experimentally measured fwhm of the incident ion beam. The final expression for comparison with the experimental data was obtained by averaging $F_i(E)$ in eq 4 over the beam distribution in eq 5.

We now believe that our assumption that E_{surf} could be described by a simple function that gives a single, discrete value for a given energy E is too simple; the variation of the impact parameter and geometry between the ion and the surface dictates that a distribution for E_{surf} should be used instead. Molecular dynamics simulations support this argument and can be used to estimate the E_{surf} distribution.[23] In direct analogy with eq 5, we can estimate a distribution for E_{surf} as

$$P_{surf}(E_{surf}; E) = (\pi^{1/2}\Delta E_{surf})^{-1} \times \exp[-(E_{surf} - E_{surf}(E))^2/\Delta E_{surf}^2] \qquad (6)$$

where ΔE_{surf} can be estimated from the fwhm of the simulated E_{surf} distribution at the energy E.

In principle, the measured fraction of product i at the detector for a nominal beam energy E_0, denoted $EF_i(E_0)$, should be calculated by averaging $F_i(E)$ in eq 4 over both the beam energy distribution in eq 5 and the E_{surf} distribution in eq 6. Rather than carrying out this complicated double integral, however, we have simplified the calculation by assuming that the effect of the distribution in E_{surf} is equivalent to a broadening of the

TABLE 1: Values of Activation Energies A_i and Fitting Constants a_i and b_i for $SiMe_3^+ \rightarrow SiMe_x^+$, $x = 0-2$: New vs Old SID Fitting Method

fragment (i)	method[a]	A_i (eV)	E_{max} (eV)	a_i	b_i
$Si(CD_3)_2^+$	CID[b]	5.32 ± 0.28			
	SID-Old[b,c]	4.3 ± 1.1	30		
	SID-New[c]	4.0 ± 1.0	30	0.012	0.003
$Si(CD_3)^+$	CID[b]	6.58 ± 0.42			
	SID-Old[b,c]	5.6 ± 1.0	40		
	SID-New[c]	6.3 ± 1.0	40	0.035	0.013
Si^+	CID[b]	10.87 ± 0.57			
	SID-Old[b,c]	7.7 ± 1.1	70		
	SID-New[c]	9.5 ± 1.0	70	0.024	0.003

[a] SID = surface-induced dissociation. CID = collision-induced dissociation in the gas phase. [b] From Table 1 of ref 12. [c] The A_i values from SID have been adjusted upward by 1.0 ± 0.5 eV to account for an estimated initial internal energy in $Si(CD_3)_3^+$.

beam energy distribution $P(E; E_0)$. This allows us to continue to associate a fixed value of E_{surf} for each value of E, denoted $E_{surf}(E)$. Thus, we can use a revised beam distribution given by

$$P'(E; E_0) = [\pi(\Delta E^2 + \delta {E_{surf}}^2)]^{-1/2} \times \exp[-(E - E_0)^2/(\Delta E^2 + \delta {E_{surf}}^2)] \quad (7)$$

where

$$\delta E_{surf} = \Delta E_{surf}/|J|$$

and

$$J = (dE_{surf}/dE)_{E=E_0}$$

The term J is the Jacobian for the transformation from E_{surf} to E. It should be emphasized that ΔE, ΔE_{surf}, J, and δE_{surf} are all considered to be functions of the nominal beam energy E_0 (rather than of E, for example), and they must be reevaluated at each new value of E_0. The final expression for $EF_i(E_0)$ is then calculated as

$$EF_i(E_0) = \int_0^\infty dE\, P'(E; E_0)\, f_i[E - E_{surf}(E)] \quad (8)$$

This is the actual expression we use here to analyze our data. We expect the approximation used to derive eq 8 to be a good one particularly because we have only a rough estimate of ΔE_{surf} (see Appendix for details).

We tested the new SID data analysis method by reevaluating the previously published activation energies A_i for SID of $SiMe_3^+$ to form $SiMe_x^+$, $x = 0-2$.[12] The distribution of energy deposited into the surface, ΔE_{surf}, was obtained from trajectory calculations[23] to be

$$\Delta E_{surf} = 0.085 E_{surf} + 0.41 \text{ eV} \quad (9)$$

All other aspects of the analysis were kept the same as previously described.[12] The new A_i values ("SID-New") are presented in Table 1 along with the best CID values and the A_i values using the old SID fitting method ("SID-Old"). E_{max} corresponds to the maximum value of E of the ERMS data used in the analysis. The a_i and b_i values in Table 1 are the Taylor series coefficients for the new fitting method, defined in eq 3. The new fitting method produces more accurate values for the higher energy $SiMe_3^+ \rightarrow Si^+$ channel, shifting A_i upward from 7.7 eV (SID-Old) to 9.5 eV (SID-New), in much better agreement with the literature CID value of 10.87 eV. The $SiMe^+$ channel from the new method is also shifted upward to a more accurate value. The $SiMe_2^+$ value is actually shifted slightly downward. Overall, inclusion of ΔE_{surf} and the Taylor series expansion renders the new SID fitting method more reliable and accurate than the old method.

IV. Computational Details

Classical dynamics simulations that model ion−surface scattering have been described fully in a separate paper and are only summarized here.[23] $C_4H_4S^+$ scattering from the C_6 surface was simulated by the chemical dynamics program *Venus 95*.[25] The Au(111) substrate model consisted of a 6×8 plane of gold atoms anchored from below by a single, strongly bound dummy atom to provide surface rigidity. Fourteen hexanethiolate adsorbates were arranged in a $(\sqrt{3} \times \sqrt{3})R30°$ overlayer on the substrate. Minimization of the slab's potential energy resulted in an average carbon chain tilt of 26° from the surface normal, in agreement with experimental results.[26,27] *Gaussian94*[28] calculations using the 6-31G* basis showed that the initial $C_4H_4S^+$ geometry was planar. The calculations were also used to determine force constants and vibrational frequencies for the cation. The initial internal energy was calculated at the beginning of each trajectory from a Boltzmann thermal population. Purely repulsive Born−Mayer type potential functions were employed to represent scattering interactions.[29,30] All $-CH_3$, $-CH_2$, and $-CH$ groups on both the ion and the surface were treated as united atoms in these calculations. These simulations did not treat fragmentation, charge exchange, or electronic excitation. A quantity of 400 trajectories were used for each collision energy, averaging over azimuthal directions corresponding to 0°, 90°, 180°, and 270° with respect to the average C_6 tilt direction. Azimuthal averaging is necessary since the ~1 cm diameter ion beam interacted with many microscopic domains of the monolayer in the experiment.[23]

V. Results

Scattered ion mass spectra of $C_4H_4S^+$ off C_6/Au(111) were examined over the energy range 5−30 eV, although the individual mass spectra are not shown here. These data indicated that surface-induced dissociation (SID) of $C_4H_4S^+$ produced three major fragment ions here: $C_2H_2S^+$, CHS^+, and $C_3H_3^+$. The total relative abundance of the parent ion and these three fragments was over 95% of the total scattered ion signal in SID. These three fragment ions also dominated the previously published threshold photoelectron photoion coincidence (TPEPICO) spectra,[6] charge exchange,[31] and conventional electron impact ionization mass spectra.[32] Therefore, we used only these four ions including the parent ion for our data analysis and ignored the other minor fragment ions. Figure 1 shows the energy-resolved mass spectra (ERMS) or plot of the scattered ion relative abundances versus the incident ion kinetic energy. Figure 1 indicates that the $C_2H_2S^+$ ion (m/z 58) was the lowest energy fragmentation channel formed by SID while the $C_3H_3^+$ ion (m/z 39) was the highest energy fragmentation channel. A similar order in appearance energy was observed for these fragments in the photoionization efficiency curve recorded by TPEPICO. However, the CHS^+ ion (m/z 45) appeared at slightly higher energies than the $C_3H_3^+$ ion (m/z 35) in SID whereas the reverse trend was observed in TPEPICO. Figure 1 also shows the SID onset energy for $C_2H_2S^+$ (m/z 58) was ~ 5 eV, while those for CHS^+ ion (m/z 45) and $C_3H_3^+$ (m/z 35) were between 8 and 9 eV.

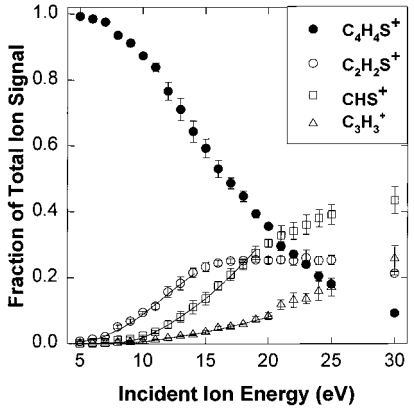

Figure 1. Experimental energy-resolved mass spectra (ERMS) of $C_4H_4S^+$ scattered off hexanethiolate/Au(111) (points) and best calculated fit to the ERMS (lines).

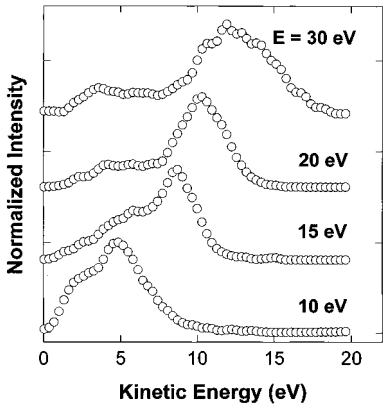

Figure 2. Kinetic energy distribution spectra (KEDS) of $C_4H_4S^+$ scattered off hexanethiolate/Au(111).

Figure 2 displays the kinetic energy distribution spectra (KEDS) of thiophene ions; this is the kinetic energy of the scattered parent ions as a function of the incident ion energy E. These KEDS were deconvoluted for the energy-dependent transmission function of the axial energy analyzer.[3] Figure 2 shows that the average energy of the scattered ion peaks increased with E. Furthermore, these peaks were broad, with 4−6 eV widths (fwhm), and these widths also increased with E. The intensities of these peaks were normalized for Figure 2; the parent ion signal actually decreased considerably from 10 to 30 eV. All the KEDS also displayed a low-energy peak or shoulder near 3−5 eV. These low-energy peaks were likely due to a distinct multiply scattered channel, and they were not included in the data analysis (see below)

We measured here activation energies of the following three fragmentation processes: $C_4H_4S^+ \rightarrow C_2H_2S^+$, $C_4H_4S^+ \rightarrow CHS^+$, and $C_4H_4S^+ \rightarrow C_3H_3^+$ by fitting the experimental ERMS data with our SID data analysis method (see Theory section above). The first step in this fitting process required knowledge of E_{surf}, the energy transferred to the surface during the ion−surface collision. E_{surf} was calculated from energy conservation before and after the ion−surface collision:

$$E = E_{int} + E_{scat} + E_{surf} \tag{10}$$

where E is now used to refer to the nominal beam energy and E_{int} and E_{scat} are the internal and kinetic energies of the scattered parent ion. E_{int} was estimated from the ERMS in Figure 1,

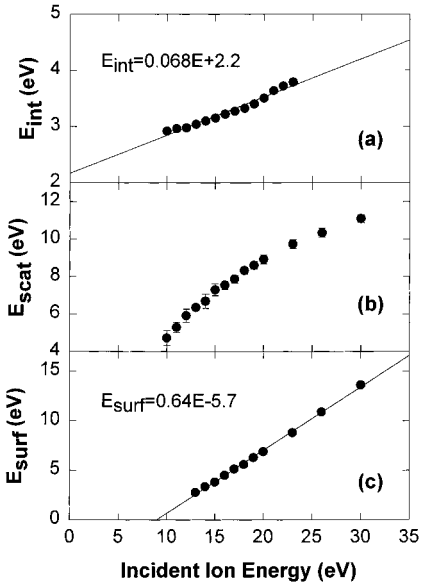

Figure 3. (a) Internal energy E_{int} for $C_4H_4S^+$ scattered off hexanethiolate/Au(111) as a function of incident ion energy. (b) Average scattered ion kinetic energy E_{scat}. (c) Energy transferred to the surface E_{surf}. Points = data; lines = best regression fit.

and E_{scat} was estimated from the KEDS in Figure 2. The exact procedures for obtaining E_{int} and E_{scat} are described below.

E_{int} as a function of E is shown in Figure 3a. We extracted E_{int} from the data points for $E = 10-23$ eV, then fit them to the following straight line.

$$E_{int} = 0.068E + 2.2 \text{ eV} \tag{11}$$

E_{int} was estimated by deconvoluting the ERMS in Figure 1 with a breakdown curve, the plot of relative abundance of fragments versus internal energy, obtained from TPEPICO.[6] The initial internal energy was estimated by consideration of the Franck Condon factors during ionization, as reflected in the TPEPICO data. The resultant 0.5 ± 0.3 eV was subtracted from each of the internal energy data points to account for the estimated initial internal energy in $C_4H_4S^+$ prior to the surface collision.[6] This method assumes that the initial internal energy is not redistributed by the surface collision. This assumption is supported by the upward shift in SID thresholds observed for internally excited ions compared with colder ions.[4] A more sophisticated means of treating initial internal energy is not yet justified given the relatively low accuracy of our initial internal energy estimate.

The KEDS in Figure 2 were used to determine the average scattered ion kinetic energies E_{scat}. KEDS data were collected with 1 eV increments between $E = 10-20$ eV and at $E = 23$, 26, and 30 eV. Next, the KEDS peaks were weight-averaged to obtain E_{scat}. Figure 3b shows the resultant E_{scat} values, indicating that they deviate from linearity at the lower E values. To avoid this nonlinearity, only data points at $E \geq 13$ eV were used to calculate E_{surf}.

E_{surf} was obtained from eq 10, and the result is shown in Figure 3c as a function of E. We previously found by examining several ion−surface pairs that E_{surf} can be described as a linear function for $E = 10-70$ eV.[2] As previously noted, the E_{surf} data for $C_4H_4S^+$ scattering off C_6/Au(111) fits this linear trend. Our data analysis model requires a functional form of E_{surf}; it was assumed to be linear in E for $E \geq 13$ eV and quadratic in E at lower energies. Justification of the E_{surf} functional form

TABLE 2: Values of Activation Energies A_i and Fitting Constants a_i and b_i for $C_4H_4S^+ \rightarrow C_2H_2S^+$, CHS^+, and $C_3H_3^+$

fragment (i)	method[a]	A_i (eV)	E_{max} (eV)	a_i	b_i
$C_2H_2S^+$	SID	4.6 ± 0.7	14	0.0026	0.0056
	TPEPICO[b]	3.23 ± 0.1			
	CE[c]	3.5 ± 0.2			
	EI[d,e]	1.9 ± 0.2			
CHS^+	SID	6.9 ± 0.7	19	0.00079	0.018
	TPEPICO[b]	4.32 ± 0.04			
	CE[c]	4.0 ± 0.2			
	EI[d]	4.1 ± 0.2			
$C_3H_3^+$	SID	6.5 ± 0.7	20	0.00049	0.004
	TPEPICO[b]	4.19 ± 0.05			
	CE[c]	4.0 ± 0.2			
	EI[d]	4.0 ± 0.2			

[a] SID = surface-induced dissociation. TPEPICO = threshold photoelectron photoion coincidence. CE = charge exchange mass spectrometry. EI = electron impact mass spectrometry. [b] From ref 6. [c] From ref 31. [d] From ref 32. Activation energies of each fragment are estimated by subtracting appearance potentials of each fragment by this experiment from the widely accepted thiophene ionization potential of 8.86 eV. [e] The activation energy of 1.9 ± 0.2 eV for the formation of $C_2H_2S^+$ by electron impact is unreasonably low when compared with those of other methods.

has been discussed previously.[12] The functional form of E_{surf} calculated this way is given by

$$E_{surf} = 0.638E - 5.73 \qquad E \geq 13 \text{ eV}$$

$$= 0.0152E^2 \qquad E < 13 \text{ eV} \tag{12}$$

As mentioned in the Theory section, E_{surf} was previously treated as a discrete value or δ function. We introduced here a width for E_{surf} known as ΔE_{surf}. We have obtained ΔE_{surf} directly from the results of the molecular dynamics simulations.

$$\Delta E_{surf} = 0.103E_{surf} + 0.287 \text{ eV} \tag{13}$$

The results of these simulations are discussed further below.

Having obtained values for E_{surf}, we then fit our ERMS data in Figure 1 using the method described in the Theory section. The curves resulting from this fitting process are shown as the solid lines overlying the data in Figure 1. Table 2 shows that the calculated activation energies for the formation of the $C_2H_2S^+$, CHS^+, and $C_3H_3^+$ ions from $C_4H_4S^+$ by SID are 4.6 ± 0.7, 6.9 ± 0.7, and 6.5 ± 0.7 eV, respectively. Our results are ~50% higher than the corresponding TPEPICO values of 3.23, 4.32, and 4.19 eV, respectively, and higher than the values from other mass spectrometry methods. Also shown in Table 2 are the best-fitting parameters a_i and b_i (defined in eq 3) and the maximum E of the fitted ERMS data E_{max}.

The partitioning of energy between the ion and the surface as predicted by classical dynamics simulations is shown in Figure 4. Simulated and experimental values of E_{int}, E_{scat}, and E_{surf} are plotted along with the experimental data in parts a, b, and c of Figure 4, respectively. These three quantities were calculated independently. The bars included in the calculated data represent the fwhm of the respective energy distribution at that E. The simulated values of E_{int}, E_{scat}, and E_{surf} are all linear in E over the entire energy range. The partitioning of E into these three energy channels is 10% into E_{int}, 12% into E_{scat}, and 78% into E_{surf}. The experimental E_{scat} data is fit with a line through the origin. The experimental E_{int} and E_{surf} data are fit with the functions in eqs 11 and 12. The average experimental partitioning of E is 23% into E_{int}, 42% into E_{scat}, and 33% into E_{surf}. The plots show semiquantitative agreement

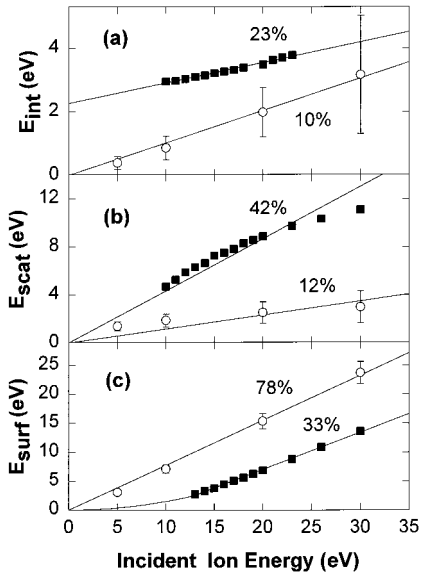

Figure 4. (a) E_{int}, (b) E_{scat}, and (c) E_{surf} from $C_4H_4S^+$ scattered off hexanethiolate-covered Au(111) as a function of incident ion energy: simulation points (○); experimental points (■). See text for description of lines.

of the simulations with the experimental data over $E = 10-30$ eV. However, the simulations overestimate the energy transfer to the surface and consequently underestimate the energy transfer to the ion translational and internal modes. It should be noted that E_{surf} is the energy transferred to an initially "cold" surface, since the inclusion of room temperature thermal energy is not expected to significantly influence energy transfer here.[23,33]

The values of ΔE_{surf} used for analysis of the SID data were obtained from the simulations (fwhm from the error bars on the points in Figure 4c). The simulations predict that ΔE_{surf} and the width of E_{scat} are both several electronvolts and scale with E. We do not have a direct experimental measure of ΔE_{surf}. However, since most of the incident energy E is channeled between E_{surf} and E_{scat},[2,23] the width of the KEDS is representative of ΔE_{surf}. As noted above, the KEDS widths are several electronvolts and increase with E. Thus, the KEDS widths indicate that the values of ΔE_{surf} derived from the molecular dynamics simulations are reasonable.

VI. Discussion

The activation energies for the formation of $C_2H_2S^+$, CHS^+, and $C_3H_3^+$ from $C_4H_4S^+$ are listed in Table 2 as 4.6 ± 0.7, 6.9 ± 0.7, and 6.5 ± 0.7 eV, respectively. Our activation energy results follow the trend in the TPEPICO values but are ~50% higher than those values and the values reported by other mass spectrometry methods.

To analyze SID data accurately, the energy distribution of both the ion kinetic energy and the energy transferred to the surface must be taken into account. The experimental ion energy distribution ΔE ranged from 2.6 to 3.7 eV and must be considered because a different initial energy E leads to a different E_{int} for constant kinetic to internal energy transfer.[17] The distribution in the energy transferred to the surface, ΔE_{surf}, arises from variations in collision geometry and impact parameter for different ion−surface collisions. This fluctuation in E_{surf} must be accounted for here because it leads to a fluctuation in the energy available for internal excitation at fixed E. Our analysis indicates that the use of average values for energy transfer will tend to overestimate the activation energies obtained

by SID.[14] These arguments are completely analogous to those used in the analysis of low-energy gas-phase collision-induced dissociation (CID) data.[34]

Our overestimation of the activation energies is due mostly to delayed dissociation of the thiophene parent ion. This kinetic shift requires an ion to absorb energy in excess of its fragmentation threshold to dissociate within the experimental time scale. The deposition of excess energy in turn leads to an overestimation of the activation energy.[5,15,22,35] We have previously described a simple analysis of KEDS data that dictates that unimolecular dissociation dominates in SID if the scattered parent ion and fragments have similar velocities for constant E, while dissociation at the surface dominates if they have similar kinetic energies.[16] Comparison of the KEDS data for the parent ion in Figure 2 with those of the fragments (data not shown) indicated a similar average velocity for all scattered ions at constant E. Thus, we concluded that unimolecular dissociation dominated for thiophene ion SID. Unimolecular decay rates were previously calculated from TPEPICO for the formation of $C_2H_2S^+$ from thiophene.[6] Using these decay rates and taking into account the detection time scale in our instrument, we found that 40% of the thiophene ions remained intact at the detector for $E = 10$ eV, 7% remained intact at $E = 13$ eV, and only 0.3% remained intact at $E = 17$ eV. Since the thresholds for formation of all these fragment ions occurred below 10 eV, the delayed dissociation effect was significant here. Therefore, we concluded that delayed dissociation was the major contribution to our overestimation of the activation energies by SID. However, this analysis did not take into account the possibility of different dissociation dynamics for SID compared with gas-phase excitation. In principle, one could attempt to model the delayed dissociation in the theoretical analysis by using additional terms in the Taylor series expansion in eq 3.

Our SID activation energies may have also been shifted upward by a nonimpulsive contribution to the internal excitation process. E_{int} was previously found to be linearly dependent on E over a wide range of energies (10−70 eV).[3,15,17,23] Our E_{int} function was also linear in this energy range, but we cannot eliminate the possibility that E_{int} is nonlinear at $E < 10$ eV. We previously argued that impulsive excitation generally dominates for nongrazing incident SID of polyatomic ions with $E = 10-70$ eV.[16] Equation 11 indicates that ∼2 eV was transferred to the scattered ions even at zero incident energy. This apparent nonimpulsive excitation might be attributed to electron transfer into a neutral excited state of thiophene on the incoming trajectory followed by reionization of the excited neutral on the outgoing trajectory. This explanation was also given for the similar effect observed for $SiMe_3^+$ scattered off clean gold.[3] Nonimpulsive excitation would render the conservation of energy equation (eq 10) invalid, leading to an underestimation of E_{surf} and an overestimation of A.

Alternatively, the E_{int} function provided in eq 11 may not represent the correct excitation function for $E < 10$ eV. Instead, the internal excitation process may be nonlinear in this low-energy regime, as is assumed here for the surface excitation process. The interaction of the ion with its image charge and with the chemisorption potential at the surface becomes most significant below $E = 10$ eV; in this case, the effect upon the kinetic-to-internal energy transfer is complex and beyond the scope of this study. Our data are not sufficiently accurate to distinguish between nonlinear and nonimpulsive excitation below 10 eV (see below). The average channeling of collision energy E into internal energy E_{int} is ∼23%, in good agreement with other literature values.[1−4,13−17,23]

The high activation energies may also have been affected by the limited energy resolution of our apparatus. The experimental uncertainties in E and ΔE were both ±1 eV owing to the use of a planar grid retarding field analyzer, while the uncertainty for E_{scat} was ±0.5 eV.[12] These uncertainties were the chief source of uncertainty in the activation energies quoted in Table 2. Furthermore, the incident ion energy E and its width ΔE are always >1 eV in any SID experiment, owing to interaction of the ion with its image charge in the surface and possibly to neutralization/reionization of the ion near the surface. Until these errors can be minimized further, there is little justification for the measurement of SID data points at energy increments smaller than 1 eV.

Our conservation of energy method used here to obtain E_{surf} (see eq 10) assumes that unimolecular dissociation dominates the scattering event. For unimolecular dissociation, the scattered parent and fragment ions will have the same velocity, allowing the use of the fragment ERMS to estimate the internal energy. If dissociation occurs on the surface, then this assumption fails and the E_{surf} function must be determined by another method. However, the model can otherwise accommodate dissociation at the surface. Overall, the method of determining E_{surf} is the weak point in our analysis and the subject of continued research.

We have seen no evidence that our use of approximate ΔE_{surf} values from the molecular dynamics simulations has affected the accuracy of our thiophene activation energies. Rather, reducing ΔE_{surf} to 50% of its initial value shifted the activation energies by less than 0.1%. Furthermore, our estimated ΔE_{surf} values are consistent with the experimentally observed ΔE_{scat} values.

In any threshold process, including the gas-phase collision-induced dissociation process upon which our model is based, there is zero probability of observing the process at threshold. Our collisional model already takes into account extrapolating down to zero probability dissociation at threshold, where the impact parameter is zero. However, our model does not take into account charge transfer. A neutralization/reionization event would require that the scattered ions have at least a kinetic energy in excess of the difference in the ionization potential of the thiophene molecule and the work function of the surface; this would shift the threshold above that predicted by our model. Although neutralization/reionization is reasonable for ion scattering off a clean metal surface, our hexanethiolate-covered targets might be better described as a metal covered with a dielectric layer. An alternative model of charge transfer for a dielectric layer is that the observed ions constitute the fraction that is not neutralized yet remain ionized throughout the scattering event. We have not included charge transfer in our model until we know more about how charge transfer occurs in these systems.

The molecular dynamics simulations for $C_4H_4S^+/C_6/Au(111)$ scattering are consistent with our previous simulations insofar as they demonstrate (1) the linear dependence of E_{scat}, E_{int}, and E_{surf} upon E and (2) the relative magnitude of these energy channels.[23] These simulations support the interpretation of hyperthermal ion−surface collisions as predominantly impulsive interactions in which collision times are on the same time scale as the vibrational periods of the colliding species; the entire ion−surface "hard spheres" interaction is complete within 300 fs, and the initial impulsive excitation on the incoming trajectory occurs in only a fraction of this time. The widths in the distributions correspond to summing over collisions of different impact parameter and geometry. These widths scale with incident energy E because these different collision conditions

are spread over a wider energy space at higher E. Also, the incident ions have energetically different collisions, since the incident ions penetrate more into the surface at higher E.

The discrepancies between the simulations and the experimental data may result partly from approximations used in the scattering model. The simplified treatment of the CH groups in thiophene as united atoms leads to fewer available internal modes for energy uptake by the scattered ion. Omission of concerted ring modes involving hydrogen atom motion may have artificially lowered E_{int}. The united atom assumption also precluded treatment of hydrogen rearrangement on the carbon ring during fragmentation, although its rearrangement may indeed have affected the energy partitioning. The simulations also did not take into account nonimpulsive excitation mechanisms such as charge exchange or electronic excitation. All scattering potentials were developed for the ground state of the interacting species. Nonimpulsive excitation may have been a minor contribution to thiophene SID, as discussed above.

Given that the simulations neglected attractive forces between the ion and surface, the overall accuracy was limited to cases in which the collision energy was greater than ~5 eV. van der Waals type attraction constituted the primary source of ion−surface attraction and has been estimated for the polyatomic ion $SiMe_3^+$ and the C_6 surface to be less than 1 eV.[23] For such weak attractive contributions, it is to be expected that the short-range, repulsive forces dominate the ion−surface interaction. This is upheld by the prediction of linear scaling of E_{surf} and E_{int} [18] for collision energies above 5 eV, which is consistent with experimental data[2] and classical dynamics simulations on other systems.[23,36] In our case, the agreement between calculated and experimental final energies is only semiquantitative, since the simulation results show relatively low E_{scat} and E_{int} values and therefore lead to higher E_{surf}. Better agreement might be obtained by actually fitting the parameters in the exponential repulsions between the ion and surface instead of using Born−Mayer parameters. However, this would only be an exercise in fitting and would not result in any augmentation of knowledge about the physical processes occurring in the system.

VII. Conclusion

We have improved our method for extracting activation energies of fragmentation for polyatomic ions from surface-induced dissociation (SID) data. Our method analyzes the energy-resolved mass spectra and the kinetic energy distribution spectra of the parent and fragment ions that scatter off the surface. It extracts the activation energies by integrating over the distribution of the initial ion energy and the energy transferred to the surface, taking into account both the average value and the widths of these distributions. The improved method was tested for $SiMe_3^+ \rightarrow SiMe_x^+$ ($x = 0-2$) fragmentation at hexanethiolate-covered gold surfaces. The new activation energies for formation of $SiMe_x^+$ were within 1.3 eV of the accepted literature values, in much better agreement than calculated by the previous version of our method.[12]

We then used our data analysis method to analyze the activation energies for the fragmentation of thiophene ions at the hexanethiolate-covered gold surface. The activation energies for the formation of $C_2H_2S^+$, CHS^+, and $C_3H_3^+$ from $C_4H_4S^+$ are 4.6 ± 0.7, 6.9 ± 0.7, and 6.5 ± 0.7 eV, respectively. Our activation energy results follow the trend in the TPEPICO values from the literature, but the SID values are ~50% higher than those from TPEPICO.[6] This discrepancy mostly results from delayed dissociation; ~40% of the thiophene ions did not dissociate during the time scale of the experiment at incident ion energies near the dissociation threshold. Analysis of the kinetic energy distribution spectra of the thiophene parent and fragment ions supports this delayed dissociation argument.

Our data and accompanying molecular dynamics simulations indicate that the impulsive excitation dominates for SID of nongrazing incidence polyatomic ions at 10's of eV collision energies, as previously argued.[3,12,16,23]

This model may be used to extract quantitative activation energies from SID data once certain ongoing issues are resolved in future papers. These unresolved issues include charge transfer, initial internal energy of the ions, determination of E_{surf}, and dissociation dynamics. Our SID data analysis method will probably never allow the determination of activation energies of small ion fragmentation that are as accurate as can be obtained by existing methods.[6−11] However, our goal is to develop SID for the determination of activation energies of fragmentation of biomolecular and other large polyatomic ions. The determination of thermochemical information on large ions remains challenging. Despite the delayed dissociation effect observed here for thiophene ions, SID appears to have unique collision dynamics that might avoid the delayed dissociation problem for large ions.[16] These unique SID collision dynamics will be discussed in future work.

Acknowledgment. This research was funded by the National Science Foundation (CHE-9457709 and CHE-9632517). L.H. is supported by a National Science Foundation Young Investigator Award (1994−1998).

Appendix

A proper calculation of $EF_i(E_0)$, the measured fraction of product i at the detector for a nominal beam energy E_0, is obtained by averaging $F_i(E)$ in eq 4 over both the beam distribution in eq 5 and the E_{surf} distribution in eq 6:

$$EF_i(E_0) = \int_0^\infty dE \int_0^\infty dE_{surf}\, f_i[E - E_{surf}(E)] \times P(E; E_0) P_{surf}(E_{surf}; E) \quad \text{(A1)}$$

Instead of carrying out this double integral, we have simplified the calculation by making two assumptions. First, we have assumed that the relationship between $E_{surf}(E)$ and E can be approximated over a narrow energy range by

$$E_{surf}(E) = \alpha E + \beta \quad \text{(A2)}$$

where α and β are constants. (If the relationship is nonlinear, we approximate it as linear with $\beta = J = dE_{surf}/dE$.) The second approximation is that since both $P(E_0)$ and $P_{surf}(E_{surf}; E)$ are Gaussian functions, we assume that $f_i[E - E_{surf}(E)]$ is slowly varying and can be taken outside the inner integral over E_{surf}, using eq A2. The innermost integral over dE_{surf} now involves the product of two Gaussian functions subject to the constraint of eq A2. This is a convolution of two Gaussian functions, which yields the Gaussian function in eq 7, and the final results for $EF_i(E_0)$ is then given in eq 8.

References and Notes

(1) Cooks, R. G.; Ast, T.; Pradeep, T.; Wysocki, V. *Acc. Chem. Res.* **1994**, *27*, 316 and references therein.

(2) Hanley, L.; Lim, H.; Schultz, D. G.; Wainhaus, S. B.; Claire, P.; Hase, W. L. *Nucl. Instrum. Methods Phys. Res., Sect. B* **1997**, *125*, 218.

(3) Wainhaus, S. B.; Lim, H.; Schultz, D. G.; Hanley, L. *J. Chem. Phys.* **1997**, *106*, 10329.

(4) Dongre, A. R.; Somogyi, A.; Wysocki, V. H. *J. Mass Spectrom.* **1996**, *31*, 339.

(5) Yeretzian, C.; Beck, R. D.; Whetten, R. L. *Int. J. Mass Spectrom. Ion Processes* **1994**, *135*, 79 and references therein.
(6) Butler, J. J.; Baer, T. *J. Am. Chem. Soc*. **1980**, *102*, 6764.
(7) Rodgers, M. T.; Armentrout, P. B. *J. Phys. Chem. A* **1997**, *101*, 2614.
(8) More, M. B.; Ray, D.; Armentrout, P. B. *J. Phys. Chem. A* **1997**, *101*, 4254.
(9) Price, W. D.; Schnier, P. D.; Williams, E. R. *Anal. Chem*. **1996**, *68*, 859.
(10) McLuckey, S. A. *J. Am. Soc. Mass Spectrom*. **1992**, *3*, 599.
(11) Klassen, J. S.; Kebarle, P. *J. Am. Chem. Soc*. **1997**, *119*, 6552.
(12) Wainhaus, S. B.; Gislason, E. A.; Hanley, L. *J. Am. Chem. Soc*. **1997**, *119*, 4001.
(13) Meot-Ner, M.; Dongre, A. R.; Somogyi, A.; Wysocki, V. H. *Rapid Commun. Mass Spectrom*. **1995**, *9*, 829.
(14) Vekey, K.; Somogyi, A.; Wysocki, V. H. *Rapid Commun. Mass Spectrom*. **1996**, *10*, 911.
(15) Weis, P.; Rockenberger, J.; Beck, R. D.; Kappes, M. M. *J. Chem. Phys*. **1996**, *104*, 3629.
(16) Burroughs, J. A.; Wainhaus, S. B.; Hanley, L. *J. Phys. Chem*. **1994**, *98*, 10913.
(17) Vekey, K.; Somogyi, A.; Wysocki, V. H. *J. Mass Spectrom*. **1995**, *30*, 212.
(18) Beck, R. D.; Rockenberger, J.; Weis, P.; Kappes, M. M. *J. Chem. Phys*. **1996**, 104, 3638.
(19) Christen, W.; Even, U.; Raz, T.; Levine, R. D. *Int. J. Mass Spectrom. Ion Processes*, in press.
(20) Hendell, E.; Even, U.; Raz, T.; Levine, R. D. *Phys. Rev. Lett*. **1995**, *75*, 2670.
(21) Gislason, E. A.; Sizun, M. *J. Phys. Chem*. **1991**, *95*, 8462.
(22) Khan, F. A.; Clemmer, D. E.; Schultz, R. H.; Armentrout, P. B. *J. Phys. Chem*. **1993**, *97*, 7978.
(23) Schultz, D. G.; Wainhaus, S. B.; Hanley, L.; Claire, P.; Hase, W. L. *J. Chem. Phys*. **1997**, *106*, 10337.
(24) Wu, Q.; Hanley, L. *J. Phys. Chem*. **1993**, *97*, 2677.
(25) Hase, W. L.; Duchovic, R. J.; Hu, X.; Lim, K. F.; Lu, D. H.; Peslherbe, G. H.; Swamy, K. N.; Vande Linde, S. R.; Wang, H.; Wolf, R. J. *Venus 95: A General Chemical Dynamics Computer Program*; Wayne State University: Detroit, MI, 1995.
(26) Hautman, J.; Klein, M. *J. Chem. Phys*. **1989**, *91*, 4994.
(27) Dubois, L. H.; Zegarski, B. R.; Nuzzo, R. G. *J. Chem. Phys*. **1993**, *98*, 678.
(28) Frisch, M. J.; et al. *Gaussian 94*, Revision A.1; Gaussian, Inc.: Pittsburgh, PA, 1995.
(29) Abrahamson, A. A. *Phys. Rev*. **1969**, *178*, 76.
(30) Meinander, N.; Tabisz, G. C. *J. Chem. Phys*. **1983**, *79*, 416.
(31) Tedder, J. M.; Vidaud, P. H. *J. Chem. Soc., Faraday Trans. 2* **1980**, *76*, 1516.
(32) Khvostenko, V. I. *Russ. J. Phys. Chem. (Engl. Transl.*) **1962**, *36*, 197.
(33) Brenner, D. W.; Harrison, J. A.; White, C. T.; Colton, R. J. *Thin Solid Films* **1991,** *206*, 220.
(34) Armentrout, P. B. In *Advances in Gas Phase Ion Chemistry*; Adams, N., Babcock, L. M., Eds.; JAI Press Inc.: Greenwich, CT, 1992; Vol. 1, p 83.
(35) Loh, S. K.; Hales, D. A.; Lian, L.; Armentrout, P. R. *J. Chem. Phys*. **1989**, *90*, 5466.
(36) Martin, J. S.; Feranchak, B. T.; Morris, J. R.; Greeley, J. N.; Jacobs, D. C. *J. Phys. Chem.* **1996**, *100*, 1689.